World Journal of Gastroenterology

Submit a Manuscript: http://www.f6publishing.com

World J Gastroenterol 2018 August 7; 24(29): 3260-3272

DOI: 10.3748/wjg.v24.i29.3260

ISSN 1007-9327 (print) ISSN 2219-2840 (online)

ORIGINAL ARTICLE

Basic Study

Downregulation of Hes1 expression in experimental biliary atresia and its effects on bile duct structure

Rui-Zhong Zhang, Xin-Hao Zeng, Ze-Feng Lin, Ming-Fu, Yan-Lu Tong, Vincent CH Lui, Paul KH Tam, Jonathan R Lamb, Hui-Min Xia, Yan Chen

Rui-Zhong Zhang, Xin-Hao Zeng, Ze-Feng Lin, Ming-Fu, Yan-Lu Tong, Hui-Min Xia, Yan Chen, Department of Pediatric Surgery, Guangzhou Women and Children's Medical Center, Guangzhou Medical University, Guangzhou 510623, Guangdong Province, China

Vincent CH Lui, Paul KH Tam, Yan Chen, Department of Surgery and Pathology, University of Hong Kong, Hong Kong, China

Jonathan R Lamb, Department of Life Sciences, Faculty of Natural Sciences, Imperial College London, London SW7 2AZ, United Kingdom

ORCID number: Rui-Zhong Zhang (0000-0002-4954-7192); Xin-Hao Zeng (0000-0002-3879-9810); Ze-Feng Lin (0000-0001-7532-9175); Ming-Fu (0000-0003-1400-0258); Yan-Lu Tong (0000-0003-0650-1562); Vincent CH Lui (0000-0002-1758-8854); Paul KH Tam (0000-0001-6231-3035); Jonathan R Lamb (0000-0002-5497-392X); Hui-Min Xia (0000-0002-0103-1672); Yan Chen (0000-0002-2354-230X).

Author contributions: Zhang RZ, Zeng XH and Lin ZF contributed equally to this work; Zhang RZ, Lin ZF and Fu M performed the animal work; Lin ZF and Tong YL analyzed the immunohistochemistry; Lui VC, Tam PK, Lamb JR, Xia HM and Chen Y contributed to the study design, data collection, analysis, discussion and manuscript preparation.

Supported by the Science and Technology Project of Guangzhou, No. 201707010014; and the National Natural Science Foundation of China, No. 81600399 and No. 81671498.

Institutional review board statement: This study was reviewed and approved by the Institutional Review Board of Guangzhou Women and Children's Medical Center, Guangzhou, China, No. 2015090109.

Institutional animal care and use committee statement: All animal protocols were approved by the Institutional Animal Care and Use Committee of Guangzhou Medical University, Guangzhou, China, No. 2016-007.

Conflict-of-interest statement: The authors declare that there is no conflict of interest related to this study.

Data sharing statement: No additional data are available.

ARRIVE guidelines statement: In the manuscript, the ARRIVE Guidelines have been adopted.

Manuscript source: Unsolicited manuscript

Correspondence to: Yan Chen, PhD, Honorary Research Felllow, Senior Scientist, Department of Surgery and Pathology, University of Hong Kong, 21 Sassoon Road, Pokfulam, Hong Kong, China. ychenc@hku.hk
Telephone: +86-852-28199602
Fax: +86-852-28199621

Received: April 23, 2018
Peer-review started: April 23, 2018
First decision: May 9, 2018
Revised: June 3, 2018
Accepted: June 25, 2018
Article in press: June 25, 2018
Published online: August 7, 2018

Abstract

AIM

To analyze the expression and function of the Notch

signaling target gene Hes1 in a rhesus rotavirus-induced mouse biliary atresia model.

METHODS

The morphologies of biliary epithelial cells in biliary atresia patients and in a mouse model were examined by immunohistochemical staining. Then, the differential expression of Notch signaling pathway-related molecules was investigated. Further, the effects of the siRNA-mediated inhibition of Hes1 expression were examined using a biliary epithelial cell 3D culture system.

RESULTS

Both immature ($EpCAM^+$) and mature ($CK19^+$) biliary epithelial cells were detected in the livers of biliary atresia patients without a ductile structure and in the mouse model with a distorted bile duct structure. The hepatic expression of transcripts for most Notch signaling molecules were significantly reduced on day 7 but recovered to normal levels by day 14, except for the target molecule Hes1, which still exhibited lower mRNA and protein levels. Expression of the Hes1 transcriptional co-regulator, RBP-Jκ was also reduced. A 3D gel culture system promoted the maturation of immature biliary epithelial cells, with increased expression of $CK19^+$ cells and the formation of a duct-like structure. The administration of Hes1 siRNA blocked this process. As a result, the cells remained in an immature state, and no duct-like structure was observed.

CONCLUSION

Our data indicated that Hes1 might contribute to the maturation and the cellular structure organization of biliary epithelial cells, which provides new insight into understanding the pathology of biliary atresia.

Key words: Biliary atresia; Rhesus rotavirus; Hes1; EpCAM; Epithelial cells 3D culture

Core tip: Similar immature biliary epithelial cells and distorted bile ductules were observed in biliary atresia patients and a mouse biliary atresia model. Investigation of the Notch signaling pathway target gene Hes1 showed that mRNA and protein expression was reduced in mouse liver, which was partially due to reduced expression of transcriptional co-regulator RBP-Jκ. In biliary epithelial cells 3D gel culture system, the administration of Hes1 siRNA blocked the maturation and duct-like structure formation process, which resulted in the cells still being in an immature state and no duct-like structure was observed.

Zhang RZ, Zeng XH, Lin ZF, Fu M, Tong YL, Lui VC, Tam PK, Lamb JR, Xia HM, Chen Y. Downregulation of Hes1 expression in experimental biliary atresia and its effects on bile duct structure. *World J Gastroenterol* 2018; 24(29): 3260-3272 Available from: URL: http://www.wjgnet.com/1007-9327/full/v24/i29/3260.htm
DOI: http://dx.doi.org/10.3748/wjg.v24.i29.3260

INTRODUCTION

Biliary atresia (BA) is the most common cause of end-stage liver disease in infants, and it has a poor prognosis with a high fatality rate. It is characterized by persistent jaundice and progressive cholestasis that develops within weeks of birth. These symptoms are caused by progressive extrahepatic and/or intrahepatic bile duct inflammation and tissue fibrosis in both the bile ducts and the liver. Although the symptoms can be partially ameliorated by Kasai surgery and extensive post-operative care, some of the patients still develop cirrhosis and liver failure due to the progressive destruction of intrahepatic bile ducts and liver fibrosis[1]. The incidence of BA in the USA is approximately 1:15000 live births, and the incidence is even higher in Asia at approximately 1:9600 live births[2,3]. Without liver transplants, the long-term survival rate of BA is between 13% and 50%[4]. Furthermore, the etiology of the disease is not fully understood. The birth defects and inflammation associated with viral infection and subsequent anti-viral immunity, which targets biliary epithelial cells (BEC), cause apoptosis and injury to the bile ducts. This results in a failure to reestablish the biliary system and progresses as tissue fibrosis, eventually leading to BA[5].

The Notch signaling pathway plays a key role in the development and differentiation of hepatic stem cells into BECs in order to establish the biliary system[6,7]. It is composed of a family of molecules, including Notch ligands, Notch receptors, DNA binding protein RBP-Jκ and effectors, such as HES, HEY, and HERP, which mediate the biological function of Notch signaling. Mutations in the Notch ligand Jagged1 (Jag1) or receptor Notch2 in humans results in Alagille syndrome (AGS), which is characterized by biliary dysplasia and cholestasis[8,9]. Similar findings have been observed in mice expressing null alleles of Jag1 or Notch2[10], which suggests a mechanism of functional conservation. Hes1 is a target gene of the Notch signaling pathway and is essential for the tubular formation in the biliary epithelium[11] and maintenance of the characteristics of the biliary epithelium[12]. However, the effect of altered Hes1 expression in BA has not been established.

Pathological observations have suggested that the blockade of the extrahepatic bile duct is the major change in both patients with BA and the animal model of BA, and that damage to the intrahepatic bile duct further enhances bile accumulation in the liver, which promotes liver fibrosis. The number of intrahepatic biliary epithelial cells (IBECs) might differ from patient to patient, but immature cell status and malformed ductular structures were commonly observed in patient liver samples[13]. Epithelial cell adhesion molecule (EpCAM) is expressed

in the embryonic stage of liver development[14], and some studies have used it as an immature epithelial cell marker for cell isolation[15]. $CK19^+$ represents a biliary epithelial cell lineage marker. It is only weakly expressed in hepatocytes, whereas it is highly expressed in mature BECs[16,17]. Using these two markers in this study, the presence of BECs was examined in rhesus rotavirus (RRV)-inoculated neonatal BA mice. The expression levels of components of the Notch signaling pathway, notably Hes1, were detected, and the effects of Hes1 loss of function on BEC morphological changes were evaluated in 3D cell culture.

MATERIALS AND METHODS

Reagents and antibodies

The rhesus rotavirus strain MMU 18006 (RRV) was purchased from the American Type Culture Collection (ATCC, Manassas, VA, United States). The virus was amplified in MA104 cells, and the virus quantification was measured by a plaque assay method, as described previously[18]. The antibodies used for immunohistochemical analyses of mouse tissue sections were rat anti-cytokeratin 19 (CK19, clone TROMA Ⅲ) and rat anti-EpCAM (clone G8.8), both of which were purchased from DSHB (Developmental Studies Hybridoma Bank, Iowa City, IA, United States). Rabbit anti-human Hes1 and rabbit anti-human RBP-Jκ were obtained from Cell Signaling Technology (Cell Signaling Technology Danvers, MA, United States). For human tissue section staining, rabbit anti-human CK19 and rabbit anti-human EpCAM were both obtained from Santa Cruz (Santa Cruz Biotechnology, Inc. Dallas, TX, United States). The RNA extraction kit and the reverse transcription reagents were purchased from Invitrogen (Life Technologies Limited, NT, Hong Kong), and Super Real Pre-Mix SYBR green was purchased from Tiangen [Tiangen Biotech (Beijing) Co., Ltd., Beijing, China].

Human samples and pathological analysis

Clinical liver tissue samples from BA patients (n = 20) and disease controls [with choledochal cyst (CC), n = 3] were obtained from the Pathology Department of Guangzhou Women and Children's Medical Center. The data were analyzed anonymously. The diagnosis was established by both pathologists and physicians based on clinical observation during operations and a laboratory-based pathological analysis. Tissue fibrosis was demonstrated by Masson tricolor staining and Sirius Red staining (data not shown). The ages of the patients included in the study ranged from two to five months old. The experimental protocols were approved by the Medical Ethics Committee of Guangzhou Women and Children's Medical Center (2015090109).

Electron microscopy analysis

The tissues were fixed in neutral glutaraldehyde and osmic acid. After dehydration, the tissues were embedded in resin. Tissue blocks were first sectioned at 1-2 microns with glass knives using an EM UC7 ultramicrotome (Leica, Buffalo Grove, IL, United States), and a reference was used to trim the blocks for thin sectioning. The appropriate blocks were then thinly sectioned at 50-70 nm. After drying on filter paper, the sections were stained with uranyl acetate and lead citrate for contrast. After drying, the grids were then viewed on a JEM-1400 microscope (JEOL USA, Inc., Peabody, MA, United States).

Infection of neonatal mice with rhesus rotavirus

Day 12.5 pregnant Balb/c mice aged between 10 and 12 wk were purchased from Guangdong Animal Experimental Centre, maintained under specific pathogen-free conditions and housed in a room with a 12-h dark-light cycle. All of the animal protocols were approved by The Institutional Animal Care and Use Committee of Guangzhou Medical University (2016-007).

To establish an experimental model of BA, neonatal mice were intraperitoneally injected within 24 h of birth with 20 μL of either 4×10^4 PFU/mL RRV or MA104 cell culture supernatant as a control. Infected mice that died within the first two days or that were not fed by their mothers were excluded from further analysis. All appropriate measures were taken to minimize the pain and discomfort of the mice. The mice were weighed and examined daily, and, in general, the development of icterus of the skin not covered with fur and acholic stools were generally observed on days five to six after the injection, indicating a successful induction of BA. The mice were sacrificed by an overdose of pentobarbitone (200 mg/kg, i.p.). To obtain tissue samples, the animals were dissected under a microscope (Nikon SMZ1000), and the gross appearances of the livers and bile ducts were recorded. The tissues were harvested and stored at -80 ℃ for RNA/protein isolation and in 10% formalin for histological sample preparation.

Histological and immunohistochemical analysis

Mouse and human liver samples were fixed and paraffin-embedded for immunostaining. Then, 4 μm thick tissue sections were rehydrated and then stained with hematoxylin and eosin (HE) for histological analysis. For immuno-histochemistry, antigen retrieval was performed in citrate buffer [10 mmol/L, 0.01% Tween20, pH 6.0 for EpCAM or Tris-EDTA buffer (10 mmol/L Tris base, 1 mmol/L EDTA solution, pH 9.0 for CK19)], and for the removal of endogenous peroxidase, the samples were treated with 3% hydrogen peroxide. The sections were then incubated overnight at 4 ℃ in blocking solution containing primary antibodies. Blocking solution without primary antibodies only was used as a control. After undergoing appropriate secondary antibody incubation, the immunostaining was completed using a Vectastain ABC Kit (Vector Laboratories, Burlingame, CA, United States) and liquid 3,3′-diaminobenzidine (Dako). The results were analyzed using a Nikon microscope, and images were captured with NIS-Elements F4.0.

Table 1 Primers used in the experiments

Genes	5′→3′	Sequences
Mouse Jag1	Forward	TTCTCACTCAGGCATGATAAACC
	Reverse	CATCTCTGGGACGACAGAACT
Mouse Dll1	Forward	CCCATCCGATTCCCCTTCG
	Reverse	GGTTTTCTGTTGCGAGGTCATC
Mouse Notch1	Forward	CCCTTGCTCTGCCTAACGC
	Reverse	GGAGTCCTGGCATCGTTGG
Mouse Notch2	Forward	CTGTGAGCGGAATATCGACGA
	Reverse	ATAGCCTCCGTTTCGGTTGG
Mouse Hes1	Forward	CCAGCCAGTGTCAACACGA
	Reverse	AATGCCGGGAGCTATCTTTCT
Mouse β-actin	Forward	AAACTGGAACGGTGAAGGTG
	Reverse	AGTGGGGTGGCTTTTAGGAT
Human Hes1	Forward	TCAACACGACACCGGATAAAC
	Reverse	GCCGCGAGCTATCTTTCTTCA
Human β-actin	Forward	TTAGTTGCGTTACACCCTTTCTTGACA
	Reverse	CTGTCACCTTCACCGTTCCAGTTTT

Gene expression profiling using quantitative PCR

The expression levels of Notch signaling-related molecules in the livers (harvested at 7 d and 14 d) of RRV-inoculated and saline control mice were determined using qPCR. The total RNA was extracted from a portion of each liver using TRIzol (Invitrogen, Carlsbad, CA, United States) according to the manufacturer's instructions, and the extracts were treated with DNAse. cDNA was synthesized using a High Capacity cDNA Reverse Transcription Kit (Applied Biosystems, Carlsbad, CA, United States) according to the manufacturer's instructions. The primers used in the experiments are shown in Table 1, and PCR was performed with a C1000 Thermal Cycler (Bio-Rad Laboratories Co., Ltd., CA, United States).

Protein expression analysis

Protein expression levels were analyzed by Western blotting according to standard protocols, and photographs were captured using a Bio-Rad molecular Imager® Gel DocTM XR+ imaging system with Image Lab™ software. The primary antibodies against Hes1 (1:1000), RBP-Jκ (1:1000), and β-actin (1:3000) and the appropriate secondary antibodies coupled with horseradish peroxidase (Bio-Rad, Munchen, Germany) were used to label the protein bands.

3D biliary epithelial cell culture

IBECs were purchased from ScienCell (Cat. Number 5100). Epithelial Cell Medium (EpiCM, ScienCell, Carlsbad, CA, United States. 4101) and additional Epithelial Cell Growth Supplement (EpiCGS, ScienCell 4152) were used for the maintenance and growth of IBECs. The medium used for the differentiation of cells was based on Kubota's Hepatoblast Growth Medium (PhoenixSongs Biologicals, Inc. Branford, CT, United States. 06405 11002-250). For IBEC differentiation, the medium was supplemented with HGF (10 ng/mL) and VEGF (20 ng/mL) (PeproTech Asia, Rehovot, Israel). The identification of the cell type was performed by immunofluorescence staining using the following 3 antibodies: AFP (Abcam, GR201677-8, 1:200) for hepatocytes and CK19 (Santa Cruz Biotechnology, K2613, 1:200) and γ-GT (Abcam, GR304453-1, 1:300) for BECs. Goat anti-mouse Alexa Fluor® 488 secondary antibody (Life Technologies, 1613346) and DAPI (KeyGen Biotech. Co., Ltd., Nanjing, China. KGR0001) were used to visualize antibody staining and the nuclei of the cells.

For the formation of duct-like structures of IBECs in three-dimensional culture, a 4:6 (v/v) gel mixture of BD Matrigel Matrix Growth Factor Reduced High Concentration (BD, 356230) and collagen Type I Rat Tail (CORNING, 354236) was used. Cells (4×10^4) were seeded on the gel using a 15-well μ-Plate Angiogenesis plate (ibidi GmbH, Martinsried, Germany, 81506) and cultured in Kubota's hepatoblast differentiation medium for seven days. The immunofluorescence staining described above was used to show the structure and differentiation statuses.

Transfection assay

To study the interruption of gene expression, such as interruption of the Notch signaling pathway target molecule Hes1, in the IBEC 3D cell culture, Hes1 siRNA RNA and control siRNA purchased from Santa Cruz Biotechnology, Inc., were used in the cell culture and transfected into cells using Lipofectamine® RNAiMAX Reagent (Life Technologies, 13778) following the manufacturer's instructions.

Statistical analysis

The data are presented as the mean ± SEM when repeated measurements were used and as the mean ± SD when individual values were used. The statistical analysis was performed by the Mann-Whitney test when two sets of data were compared and by the Kruskal-Wallis test when more than three sets of data were compared. The statistical analysis was performed using GraphPad Prism software (GraphPad Software Inc., La Jolla, CA, United States) with P values < 0.05 taken as

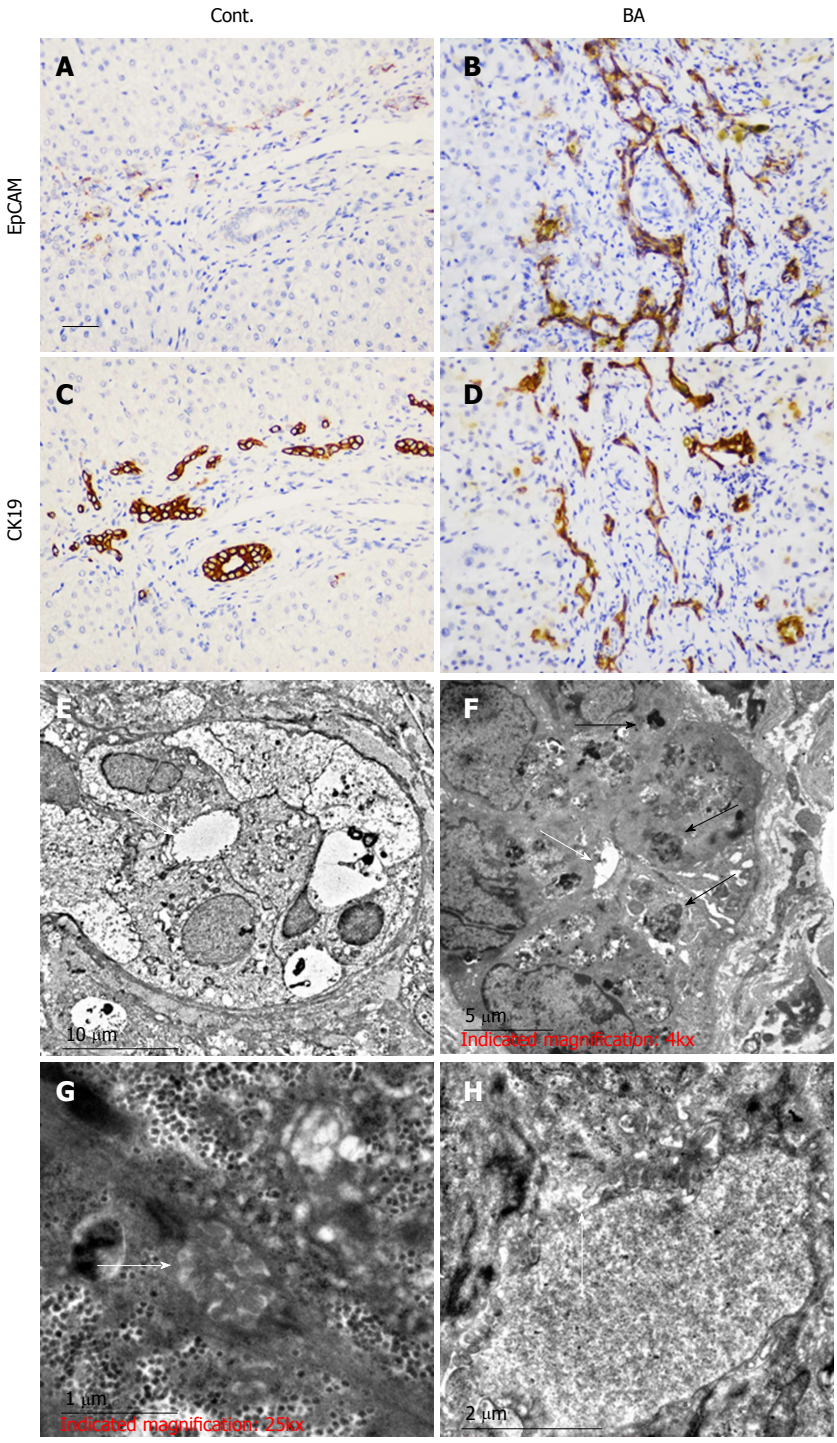

Figure 1 Expression levels of EpCAM and CK19 in neonatal liver biopsies and electron microscopy analysis of hepatic ultrastructure. To test the biliary epithelial marker expression levels, immunohistochemical staining was performed on disease control samples (Cont., choledochal cyst, A and C) and biliary atresia patient samples (BA, B and D). For the colocalization study of EpCAM and CK19, adjacent tissue sections were used. The scale bar is shown as 50 μm. For the EM analysis, liver tissues from the Cont. (E and F) and BA patients (G and H) were sectioned at 50-70 nm and stained with uranyl acetate and lead citrate. Photographs of the bile capillary (E and G) and microvilli (F and H) were captured and presented. The scale bar is also shown in the photographs. *n* = 5 each for the CC and BA groups.

the level of significance.

RESULTS

Increase in EpCAM immunopositive cells in the liver tissue of BA patients and the study of the ultrastructure of cells

We used adjacent, age-matched sections for studying immature BECs ($EpCAM^+$) and immunohistochemical staining of the BEC marker ($CK19^+$). Our results showed that compared with choledochal cysts as a control (Cont., Figure 1A and C) there were highly increased numbers of $EpCAM^+$ cells in BA (Figure 1B and D). Most $EpCAM^+$ cells were also $CK19^+$, indicating that EpCAM is expressed in BECs. In choledochal cysts, disappearance

of the EpCAM$^+$ marker indicated the mature status of the cells. Additionally, the bile ductules could be easily observed in choledochal cysts but not in BA.

The ultrastructural changes in the morphology of the bile ducts in BA patients were compared to those in CC patients. The results revealed a similar hepatic cellular ultrastructure appearance in both cases. Mild swelling of liver cells was observed with no obvious abnormalities in the nuclei, rough endoplasmic reticulum, or smooth endoplasmic reticulum, apart from slight hyperplasia. However, in the portal triad, abnormal narrowing of the bile capillary was observed together with irregular sediments of bilirubin particles in the BA group (Figure 1F) in contrast to the CC group (Figure 1E). Fewer microvilli and less bile salt deposition were found in the BA patient tissue sections (Figure 1H) than in the CC patient tissue sections (Figure 1G). Taken together, these data suggest that BECs in BA patients are not fully mature, which might affect bile transport.

Optimization of the dose of rhesus rotavirus for the induction of BA in mice

Viral infection is proposed to be a causative factor in the development of BA, and the RRV-induced BA mouse model is used to mimic the pathophysiological processes in human BA. However, high doses of virus (1×10^6 PFU/mL) often cause the early death of mice at days 5-7 after viral inoculation. To reduce mortality, we used a smaller dose of RRV (4×10^4 PFU/mL) to induce BA. After viral inoculation, the mice exhibited BA syndrome with jaundice (Figure 2A) and extrahepatic bile duct occlusion (Figure 2B). The survival rate with this dosage was 63.03% and significantly differed from that of the control group (supernatant without virus infection) (Figure 2C; $P < 0.05$). Changes in weight loss were significant, with the control group exhibiting a 10.0 g $\pm$ 0.25 g change ($n = 15$) but the RRV-treated group only exhibiting a 5.6 g $\pm$ 1.3 g change ($n = 26$) (Figure 2D; $P < 0.001$). After dissection and tissue sectioning of the livers of the BA mice, HE staining revealed that, in contrast to the normal control group (Figure 2E), a disappearance of the common bile duct was observed in the BA group (Figure 2F). At the portal triads, enlarged cystic ducts and inflammatory cell accumulation were also present at day 14 after RRV inoculation, in contrast to normal control mice (Figure 2H *vs* Figure 2G).

Presence of EpCAM$^+$ and CK19$^+$ bile ducts in RRV-inoculated BA mice

To identify the bile ducts, immunohistochemical staining was performed for both EpCAM and CK19 at days 7 and 14 after RRV inoculation, and RRV-inoculated mice were compared with control mice. As shown in Figure 3, EpCAM$^+$ bile ducts were noted at both days 7 and 14 in the control mice (Figure 3A and 3C), but few EpCAM$^+$ cells were found in the RRV-inoculated mouse BA livers at day 7 (Figure 3B). At day 14, more EpCAM$^+$ cells were detected, even in the areas of the portal tracts that were infiltrated with inflammatory cells. However, none of these cells were organized into ductule-like structures (Figure 3D). Similar to EpCAM, CK19$^+$ ductules were observed in the control livers at days 7 and 14, although the signal was slightly weaker on day 7 (Figure 3E and G). However, in BA mice, CK19$^+$ cells were found in the portal areas, but no ductule structures were observed (Figure 3F and H). This observation suggests the presence of BECs, especially at day 14 after RRV inoculation. However, their development, especially in the formation of the bile duct process, was interrupted.

Expression of Notch signaling pathway components in the liver tissues of RRV-inoculated BA mice

The Notch signaling pathway plays a key role in bile duct system development. To examine its function in this model, qPCR was employed to quantify the expression levels of key genes in the Notch signaling pathway. The results showed that at day 7, there was a marked reduction in the expression levels of Notch ligands [Jag1 and Delta-like (Dll1)], Notch receptors (Notch1 and Notch2), and the Notch target gene Hes1 in the BA liver tissues compared with control liver tissues (Figure 4A, $P < 0.05$ for Jag1 and Notch1, $P < 0.01$ for Hes1 compared with the control). At day 14, no obvious differences in the expression levels of Jag1, Dll1, Notch1 and Notch2 were observed between the control and BA groups, and a slight increase in the expression of Notch2 was even found, although not statistically significant ($P = 0.1434$). However, the levels of Hes1 transcripts remained significantly reduced (10-fold compared with the control; $P < 0.001$; Figure 4B). The protein expression levels were then examined using Western blotting, which yielded similar results, namely, that the concentration of Hes1 protein in the mouse BA group was significantly lower on both day 7 and day 14 after RRV inoculation than that in the control group (Figure 4C). These data suggest that BA in RRV-inoculated mice may be caused, at least partially, by the downregulation of Hes1 expression.

Downregulation of RBP-Jκ protein in the liver tissues of BA mice

As we observed reduced expression of Hes1, we then chose to investigate the expression levels of the regulators of Hes1. We determined the expression of the cotranscriptional factor RBP-Jκ by Western blotting, and the results demonstrated that there was a minimal expression of RBP-Jκ at both day 7 and day 14 in the BA mice compared to controls (Figure 4C). This finding suggests that downregulation of RBP-Jκ may be the cause of the reduced expression of Hes1 and may subsequently hinder normal bile duct development.

Hes1 siRNA in the development of duct-like structures in 3D cell culture

The function of Hes1 in bile duct development was evaluated using a Hes1 siRNA transfection assay in a BEC

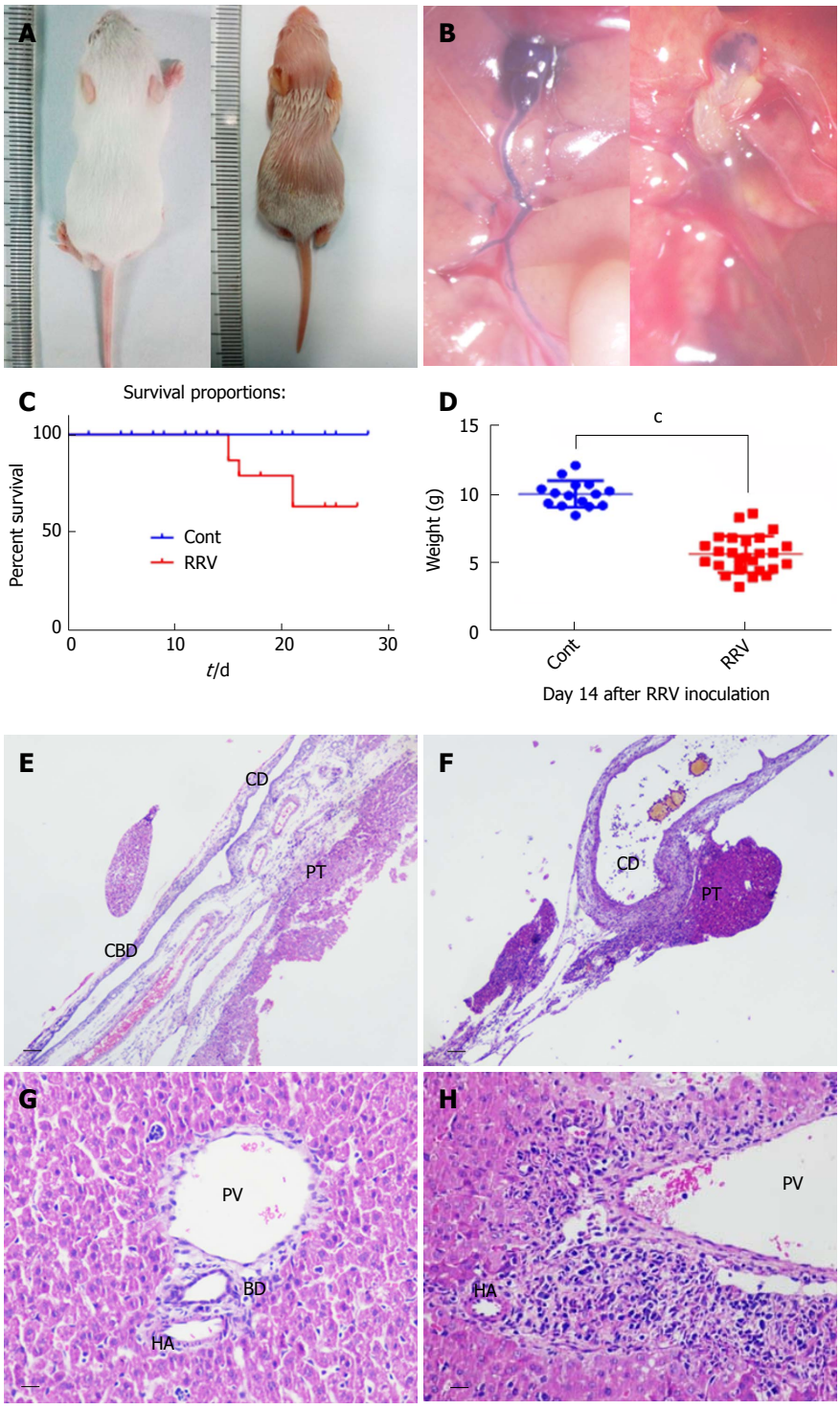

Figure 2 Biliary atresia in neonatal mice with a low dose of rhesus rotavirus inoculation. To study the expression levels of the components of the Notch signaling pathway in the biliary atresia (BA) animal model, a lower dose of 20 μL of rhesus rotavirus (RRV) with a titer of 4×10^4 PFU/mL was used. The morphology and extrahepatic block were photographed (A and B). The survival rate was measured at 21 d after viral inoculation (C). BA syndrome was observed between days 5 and 6. The body weights of the mice were measured at day 14 and compared with that of the control group (injected with culture supernatant but no virus) (D) ($P < 0.001$, $n = 15$ in the Cont. group, and $n = 26$ in the RRV group). After dissection, the portal triad (E and F) and liver tissue at day 14 (G and H) were sectioned, and histological analysis was performed. The scale bar is shown as 0.2 mm in the portal triad sections and as 50 μm in the liver tissue sections. CD: Cystic duct; CBD: Common bile duct; PT: Portal triad; PV: Portal vein; HA: Hepatic artery; BD: Bile duct.

culture. When BECs were cultured in growth medium, immunostaining showed that the cells expressed positive signals for CK19 and γ-GT but also a positive signal for AFP, which suggests the immature status of the cells (Figure 5, N. Medium). However, when the cells were cultured in matrix gel + collagen gel (the mixed gel), the cells showed positive signals only for the BEC markers CK19 and γ-GT (Figure 5, Cont.), which suggested that the maturation process was underway. The formation of cells into duct-like structures was also observed

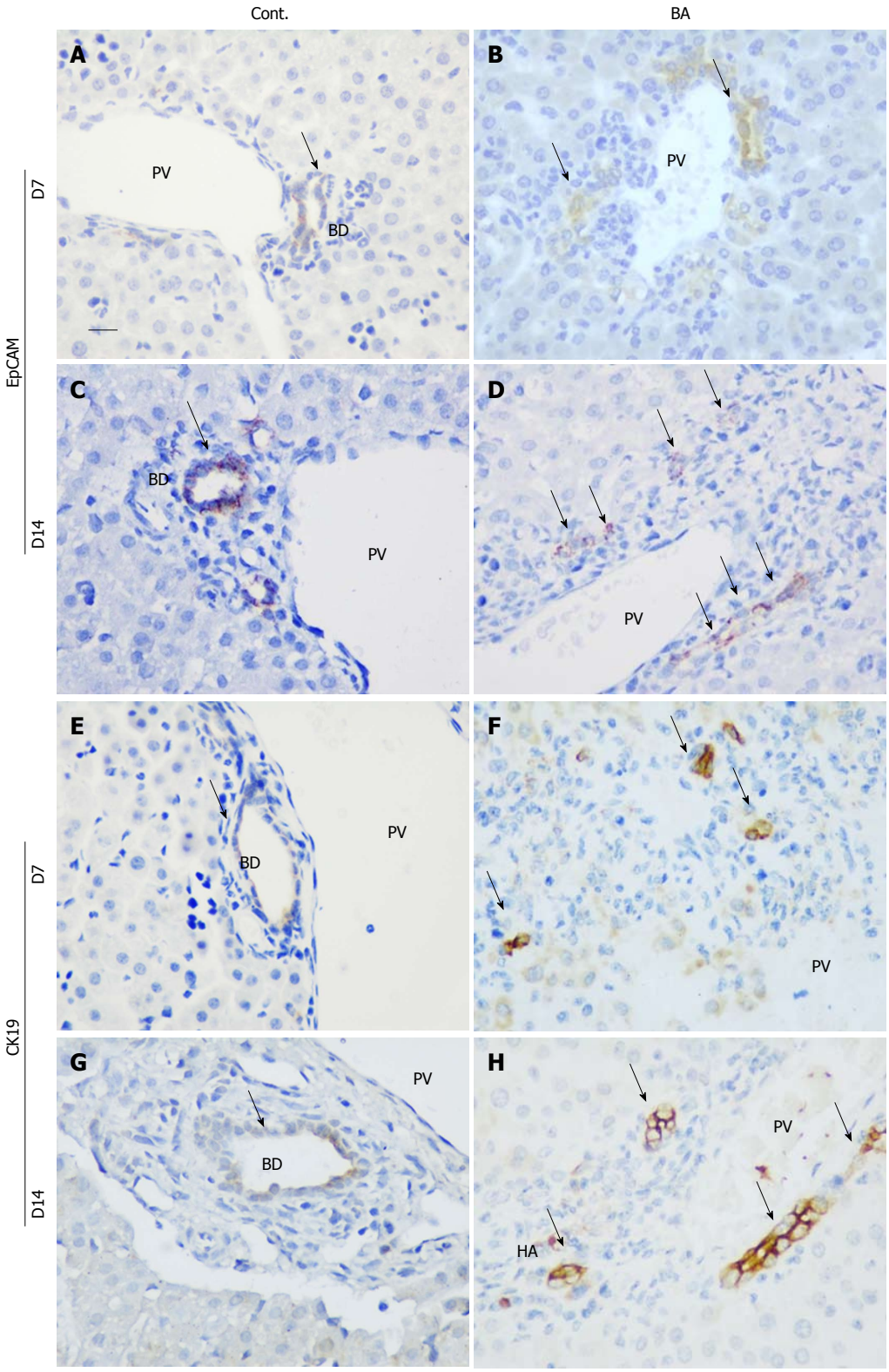

Figure 3 Expression levels of EpCAM and CK19 in the liver and ultrastructure of biliary epithelial cells. The expression levels of EpCAM and CK19 were analyzed using immunohistochemical staining with antibodies. The tissue sections were collected at day 7 (A, B, E and F) and day 14 (C, D, G and H). After they were dewaxed, the sections were stained with EpCAM and CK19 antibodies, and a comparison of the mice in the control group (Cont.) and those in the rhesus rotavirus inoculation group was performed. The scale bar shown is 100 μm. The black arrow indicates the positive signal. BA: Biliary atresia; CD: Cystic duct; CBD: Common bile duct; PT: Portal triad; PV: Portal vein; HA: Hepatic artery; BD: Bile duct.

after seven days in cell culture (Figure 5, Cont.). An enhanced density of duct-like structures was observed with prolonged culture time. These data indicated that the culture conditions promoted the maturation of cells. The low toxicity of the transfection reagent for duct-like structure formation was tested, and the results showed

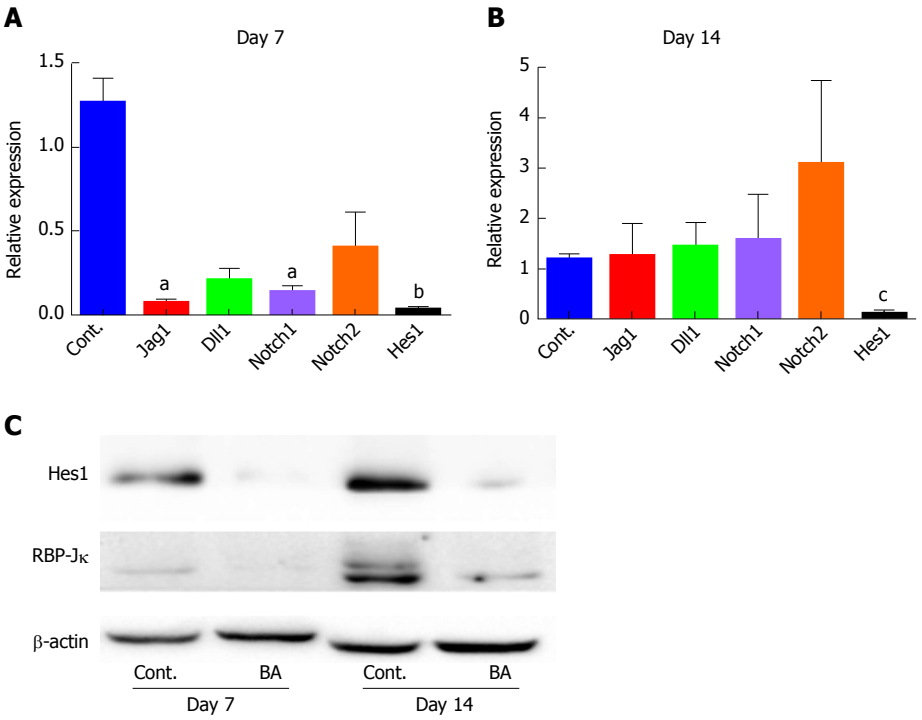

Figure 4 Expression levels of Notch signaling components in the liver of rhesus rotavirus-inoculated mice. The mRNA levels of Notch signaling components, including Jag1, Dll1, Notch1, Notch2 and Hes1, were detected using quantitative real-time PCR with appropriate primers at day 7 and day 14 after RRV inoculation. A: The relative expression levels compared with the normal control are shown for day 7 ($^{a}P < 0.05$; $^{b}P < 0.01$; $n = 6$ in the control group and $n = 10$ in the RRV group); B: day 14 ($^{c}P < 0.001$); C: The levels of the Hes1 protein and the expression of the transcriptional coregulator RBP-Jκ were detected by Western blot ($n = 2$ or 3 in each group; the proteins were mixed and loaded).

that there was no obvious difference in duct formation in the transfection reagent group (Figure 5, Lipo) compared with the control group. However, Hes1 siRNA transfection induced an obvious difference compared with the irrelevant siRNA control (Figure 5, Hes1 siRNA *vs* Cont. siRNA), as no duct-like structures were observed in Hes1 siRNA-transfected cells, and these cells were kept in an immature state according to AFP^{+} staining.

DISCUSSION

EpCAM is a cell surface-expressed transmembrane molecule that is present not only on epithelial cells but also on a variety of cells, including stem cells and cancer stem cells[19]. Using a BEC marker for colocalization, CK19, we noted that the number of EpCAM^{+} cells was increased in BA patients but not in CC control patients, suggesting active proliferation of BECs in BA. Furthermore, CK19 has been reported as a marker for ductal reactivity in tumor studies[20,21]. EpCAM expression in epithelial cells has been linked to the epithelial-mesenchymal transition (EMT)[22], but its role in this process remains controversial[23]. Both EMT and the ductal reaction are relevant to the development of tissue fibrosis[24], although the associated mechanisms have not been fully defined[25]. Elucidating EpCAM expression and its regulation in BA patients and/or experimental models of BA might provide new information regarding the relationship of the ductal reaction with tissue fibrosis, especially as some previous studies have already reported the occurrence of EMT in BA patients[26-28].

We found that EpCAM^{+} cell number was closely correlated with the expression of the Notch signaling target gene Hes1 and that Hes1 expression was increased in the nuclei of BECs in BA patients and RRV-inoculated mice. The expression of Hes1, as a nuclear regulatory protein, has been well-studied in biliary tract development, and as such, the Hes1-null mice showed a relatively normal ductal plate consisting of cytokeratin-positive and DBA-positive cholangiocyte precursors. However, by postnatal day 0, these mice presented with gallbladder agenesis and severe hypoplasia of the extrahepatic bile ducts[12], suggesting immature differentiation of BECs. In accordance with previous observations, our data of the 3D BEC cell culture also demonstrate that low levels of Hes1 prevented the formation of duct-like structures. Additionally, the increase in the expression levels of the mature BEC markers γ-GT and CK19 and the reduction in the expression of AFP are further evidence that Hes1 functions in the maturation and structural reorganization of these cells. We sought to examine the expression of Hes1 in human BA samples. Immunohistochemistry staining revealed heterogeneity in the results, even among the same tissue samples (data not shown). Thus, the Hes1 effect in BA might be related to different stages (inflammation or fibrogenesis) of the

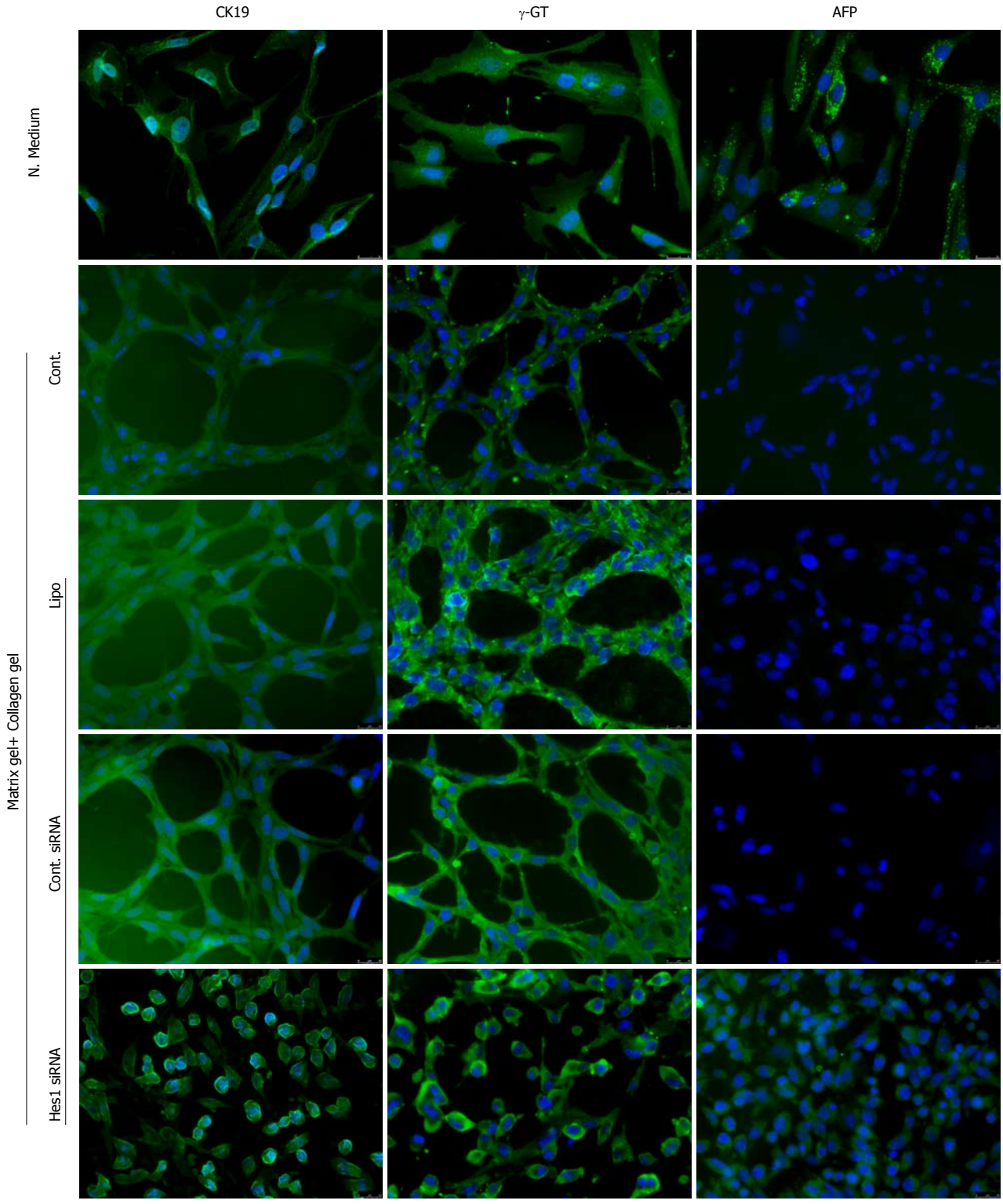

Figure 5 Hes1 siRNA in 3D biliary epithelial cell culture. Biliary epithelial cells (BECs) were cultured in either normal growth medium (N. medium) or in matrix + collagen mixed gel (detailed components are given in the Materials and Methods section). The cells were cultured without a transfection reagent (Cont.), with Lipofectamine (Lipo) only, with irrelevant control siRNA (Cont. siRNA) or with Hes1 siRNA for seven days, then fixed and stained with anti-CK19, γ-GT and AFP antibodies, and finally counter-stained with Alexa Fluor®488. Photographs of the cells were taken with a Leica DMi8 inverted fluorescence microscope, and the groups were then compared. The experiment was duplicated, and one set of representative results is shown here.

disease, as most of the BA patients in the clinic were in the stage of tissue fibrosis or later stages of the disease. Recruiting earlier-stage patients in whom inflammation is still progressing will help to clarify the alterations in Hes1 expression in BA patients.

The expression of Hes1 is under the control of coregulatory factors, particularly NICD and RBP-Jκ. NICD is a component of the Notch signaling pathway, and in our

study, its expression was relatively normal, although some intracellular signaling pathway components, such as gamma secretase, might still affect the levels of NICD[29]. Here, we provide evidence of a clear decline in the expression of RBP-Jκ, which might be the cause of reduced Hes1. A similar phenomenon was observed in RBP-Jκ KO mice. In those animals, the mature ducts were significantly reduced with respect to similarly treated wild-type mice[30]. It has been reported that RBP-Jκ expression is modulated by many regulatory factors, including viral infection[31,32]. In Epstein-Barr virus (EBV) infection, the nuclear antigens (EBNA) 3A and 3C can compete with EBNA 2 in binding with RBP-Jκ, thus inhibiting RBP-Jκ function. This diminishes the functional activity of Notch signaling by reducing the expression of Hes1[33]. However, whether or not there is any similarity between the EBV and RRV components in Hes1 expression remains to be investigated. At the end of the study, a high dose of Pentobarbital was administered to the mice, and then samples were collected for analysis. It has been shown that Pentobarbital affects bile secretion[34], however, as we used a control group, and the comparative results showed a difference between the treatment and control groups, the effect of Pentobarbital might not have directly influenced the results. Further research with mouse sacrifice by dislocation of the cervical spine will help to clarify this point.

The results of this study suggest that the reduced Hes1 expression may have contributed to reformation of the functional bile duct, but other factors cannot be excluded, such as inflammation or viral infection. The construction or adaptation of conditional knockout mice with targeted Hes1 knockdown on day 7, together with the BA mouse model with Hes1 overexpression, might help to confirm that Hes1 is the only contributing factor in this BA mouse model. The results of these experiments will provide more information regarding whether Hes1 overexpression has any therapeutic effect in the treatment of BA.

The mouse model used in this study represents acute viral infection-induced biliary atresia, in which tissue fibrosis is absent. The direct comparison of the mouse data with the patient data is not appropriate, as in patients, substantial tissue fibrosis is often observed at the later stage. Therefore, the development of a chronic BA mouse model will better mimic the condition observed in BA patients, allowing for a more accurate comparison of Hes1 data.

In conclusion, our study demonstrated that EpCAM$^+$ cells are increased in the liver tissue of BA patients and the BA mouse model. The experimental results presented here suggest that the Notch signaling effector gene Hes1 might contribute to the disease processes in BA and that downregulation of RBP-Jκ might account for the pathophysiological changes in the bile ducts that were observed in the BA mouse model. The 3D BEC culture further confirmed the effect of Hes1 on the maturation and the duct-like structural formation of cells, which helps to further explain the dysregulation of structure formation in BA patients.

ARTICLE HIGHLIGHTS

Research background

An increased number of immature biliary epithelial cells and distorted bile ductules were observed in biliary atresia (BA), but the causes of these changes are unknown. The Notch signaling pathway is related to the development and differentiation of biliary epithelial cells. The target gene Hes1 is essential for tubular formation and maintenance. However, the effect of altered Hes1 expression in biliary atresia has not been established.

Research motivation

Notch signaling is one of the main pathways involved in bile duct development. However, its function in BA is not well known. Analysis of Notch signaling molecules using an established BA animal model, and 3D cell culture system might provide novel insights into the pathogenesis of BA.

Research objectives

The expression of Notch signaling pathway-related molecules was detected in a BA mouse model. The function of Hes1 downregulation was further examined using a 3D cell culture system. The results of this study can be expanded upon in future research of human BA patients by examining Hes1 expression and its relationship with BA pathogenesis.

Research methods

Immature biliary epithelial cells and bile duct structure distortion were examined in BA patients and in a BA mouse model. The expression of Notch signaling pathway-related molecules was detected in the mouse model by qPCR, and the expression of Hes1 and its gene regulatory protein was further confirmed by Western blotting. Finally, in 3D cell culture, the effects of Hes1 inhibition induced by siRNA transfection on duct-like structure formation were observed.

Research results

The results revealed the presence of immature biliary epithelial cells and distorted structures in both the BA patients and animal model. The downregulation of Hes1 expression, together with its transcriptional co-regulator RBP-Jκ, was observed in the BA mouse model. The siRNA-mediated inhibition of Hes1 completely blocked duct-like structure formation in the 3D cell culture system. However, Hes1 expression in BA patients must be further evaluated to confirm its function in the disease process.

Research conclusions

In conclusion, the results of the current study indicate that the immature biliary epithelial cells and defective duct-like structure formation in BA might be partly related to downregulation of the expression of the Notch signaling target gene Hes1. The use of a 3D epithelial cell culture system might help to identify other potential molecules, including those involved in epithelial cell maturation and duct-like structure formation.

Research perspectives

The potential effects of Hes1 observed in the BA mouse model and cell culture involving biliary epithelial cell maturation and duct-like structure formation suggest that Hes1 might contribute to the pathogenesis of BA. However, further examination of BA patient samples is necessary to better understand the role of Hes1 in the BA disease process.

ACKNOWLEDGMENTS

The authors would like to thank Dr. Stacey Cherny of the Department of Psychiatry at the University of Hong Kong

for assisting with the statistical analysis. The authors also would like to thank the Department of Pathology and Biobank, Guangzhou Women and Children's Medical Center for providing the clinical samples.

REFERENCES

1 **Hartley JL**, Davenport M, Kelly DA. Biliary atresia. *Lancet* 2009; **374**: 1704-1713 [PMID: 19914515 DOI: 10.1016/S0140-6736(09)60946-6]

2 **Yoon PW**, Bresee JS, Olney RS, James LM, Khoury MJ. Epidemiology of biliary atresia: a population-based study. *Pediatrics* 1997; **99**: 376-382 [PMID: 9041292 DOI: 10.1542/peds.99.3.376]

3 **Davenport M**. Biliary atresia. *Semin Pediatr Surg* 2005; **14**: 42-48 [PMID: 15770587 DOI: 10.1053/j.sempedsurg.2004.10.024]

4 **Gallo A**, Esquivel CO. Current options for management of biliary atresia. *Pediatr Transplant* 2013; **17**: 95-98 [PMID: 23347466 DOI: 10.1111/petr.12040]

5 **Bessho K**, Bezerra JA. Biliary atresia: will blocking inflammation tame the disease? *Annu Rev Med* 2011; **62**: 171-185 [PMID: 21226614 DOI: 10.1146/annurev-med-042909-093734]

6 **Boulter L**, Lu WY, Forbes SJ. Differentiation of progenitors in the liver: a matter of local choice. *J Clin Invest* 2013; **123**: 1867-1873 [PMID: 23635784 DOI: 10.1172/JCI66026]

7 **Morell CM**, Strazzabosco M. Notch signaling and new therapeutic options in liver disease. *J Hepatol* 2014; **60**: 885-890 [PMID: 24308992 DOI: 10.1016/j.jhep.2013.11.028]

8 **Li L**, Krantz ID, Deng Y, Genin A, Banta AB, Collins CC, Qi M, Trask BJ, Kuo WL, Cochran J, Costa T, Pierpont ME, Rand EB, Piccoli DA, Hood L, Spinner NB. Alagille syndrome is caused by mutations in human Jagged1, which encodes a ligand for Notch1. *Nat Genet* 1997; **16**: 243-251 [PMID: 9207788 DOI: 10.1038/ng0797-243]

9 **Oda T**, Elkahloun AG, Pike BL, Okajima K, Krantz ID, Genin A, Piccoli DA, Meltzer PS, Spinner NB, Collins FS, Chandrasekharappa SC. Mutations in the human Jagged1 gene are responsible for Alagille syndrome. *Nat Genet* 1997; **16**: 235-242 [PMID: 9207787 DOI: 10.1038/ng0797-235]

10 **McCright B**, Lozier J, Gridley T. A mouse model of Alagille syndrome: Notch2 as a genetic modifier of Jag1 haploinsufficiency. *Development* 2002; **129**: 1075-1082 [PMID: 11861489]

11 **Kodama Y**, Hijikata M, Kageyama R, Shimotohno K, Chiba T. The role of notch signaling in the development of intrahepatic bile ducts. *Gastroenterology* 2004; **127**: 1775-1786 [PMID: 15578515 DOI: 10.1053/j.gastro.2004.09.004]

12 **Sumazaki R**, Shiojiri N, Isoyama S, Masu M, Keino-Masu K, Osawa M, Nakauchi H, Kageyama R, Matsui A. Conversion of biliary system to pancreatic tissue in Hes1-deficient mice. *Nat Genet* 2004; **36**: 83-87 [PMID: 14702043 DOI: 10.1038/ng1273]

13 **Zhang RZ**, Yu JK, Peng J, Wang FH, Liu HY, Lui VC, Nicholls JM, Tam PK, Lamb JR, Chen Y, Xia HM. Role of CD56-expressing immature biliary epithelial cells in biliary atresia. *World J Gastroenterol* 2016; **22**: 2545-2557 [PMID: 26937142 DOI: 10.3748/wjg.v22.i8.2545]

14 **de Boer CJ**, van Krieken JH, Janssen-van Rhijn CM, Litvinov SV. Expression of Ep-CAM in normal, regenerating, metaplastic, and neoplastic liver. *J Pathol* 1999; **188**: 201-206 [PMID: 10398165 DOI: 10.1002/(SICI)1096-9896(199906)188:2<201::AID-PATH339>3.0.CO;2-8]

15 **Joplin R,** Kachilele S. Human intrahepatic biliary epithelial cell lineages: studies in vitro. Hepatocyte Transplantation: Springer, 2009: 193-206

16 **Sekiya S**, Suzuki A. Intrahepatic cholangiocarcinoma can arise from Notch-mediated conversion of hepatocytes. *J Clin Invest* 2012; **122**: 3914-3918 [PMID: 23023701 DOI: 10.1172/JCI63065]

17 **Stamp L**, Crosby HA, Hawes SM, Strain AJ, Pera MF. A novel cell-surface marker found on human embryonic hepatoblasts and a subpopulation of hepatic biliary epithelial cells. *Stem Cells* 2005; **23**: 103-112 [PMID: 15625127 DOI: 10.1634/stemcells.2004-0147]

18 **Arnold M**, Patton JT, McDonald SM. Culturing, storage, and quantification of rotaviruses. *Curr Protoc Microbiol* 2009; **15**: Unit 15C.3 [PMID: 19885940 DOI: 10.1002/9780471729259.mc15c03s15]

19 **Dollé L**, Theise ND, Schmelzer E, Boulter L, Gires O, van Grunsven LA. EpCAM and the biology of hepatic stem/progenitor cells. *Am J Physiol Gastrointest Liver Physiol* 2015; **308**: G233-G250 [PMID: 25477371 DOI: 10.1152/ajpgi.00069.2014]

20 **Yoon SM**, Gerasimidou D, Kuwahara R, Hytiroglou P, Yoo JE, Park YN, Theise ND. Epithelial cell adhesion molecule (EpCAM) marks hepatocytes newly derived from stem/progenitor cells in humans. *Hepatology* 2011; **53**: 964-973 [PMID: 21319194 DOI: 10.1002/hep.24122]

21 **Zhang Q**, Zhang CS, Xin Q, Ma Z, Liu GQ, Liu BB, Wang FM, Gao YT, Du Z. Perinodular ductular reaction/epithelial cell adhesion molecule loss in small hepatic nodules. *World J Gastroenterol* 2014; **20**: 10908-10915 [PMID: 25152593 DOI: 10.3748/wjg.v20.i31.10908]

22 **Gao J**, Yan Q, Wang J, Liu S, Yang X. Epithelial-to-mesenchymal transition induced by TGF-β1 is mediated by AP1-dependent EpCAM expression in MCF-7 cells. *J Cell Physiol* 2015; **230**: 775-782 [PMID: 25205054 DOI: 10.1002/jcp.24802]

23 **Massoner P**, Thomm T, Mack B, Untergasser G, Martowicz A, Bobowski K, Klocker H, Gires O, Puhr M. EpCAM is overexpressed in local and metastatic prostate cancer, suppressed by chemotherapy and modulated by MET-associated miRNA-200c/205. *Br J Cancer* 2014; **111**: 955-964 [PMID: 24992580 DOI: 10.1038/bjc.2014.366]

24 **Kalluri R**, Neilson EG. Epithelial-mesenchymal transition and its implications for fibrosis. *J Clin Invest* 2003; **112**: 1776-1784 [PMID: 14679171 DOI: 10.1172/JCI20530]

25 **Williams MJ**, Clouston AD, Forbes SJ. Links between hepatic fibrosis, ductular reaction, and progenitor cell expansion. *Gastroenterology* 2014; **146**: 349-356 [PMID: 24315991 DOI: 10.1053/j.gastro.2013.11.034]

26 **Omenetti A**, Bass LM, Anders RA, Clemente MG, Francis H, Guy CD, McCall S, Choi SS, Alpini G, Schwarz KB, Diehl AM, Whitington PF. Hedgehog activity, epithelial-mesenchymal transitions, and biliary dysmorphogenesis in biliary atresia. *Hepatology* 2011; **53**: 1246-1258 [PMID: 21480329 DOI: 10.1002/hep.24156]

27 **Xiao Y**, Zhou Y, Chen Y, Zhou K, Wen J, Wang Y, Wang J, Cai W. The expression of epithelial-mesenchymal transition-related proteins in biliary epithelial cells is associated with liver fibrosis in biliary atresia. *Pediatr Res* 2015; **77**: 310-315 [PMID: 25406900 DOI: 10.1038/pr.2014.181]

28 **Deng YH**, Pu CL, Li YC, Zhu J, Xiang C, Zhang MM, Guo CB. Analysis of biliary epithelial-mesenchymal transition in portal tract fibrogenesis in biliary atresia. *Dig Dis Sci* 2011; **56**: 731-740 [PMID: 20725787 DOI: 10.1007/s10620-010-1347-6]

29 **Roncarati R**, Sestan N, Scheinfeld MH, Berechid BE, Lopez PA, Meucci O, McGlade JC, Rakic P, D'Adamio L. The gamma-secretase-generated intracellular domain of beta-amyloid precursor protein binds Numb and inhibits Notch signaling. *Proc Natl Acad Sci U S A* 2002; **99**: 7102-7107 [PMID: 12011466 DOI: 10.1073/pnas.102192599]

30 **Fiorotto R**, Raizner A, Morell CM, Torsello B, Scirpo R, Fabris L, Spirli C, Strazzabosco M. Notch signaling regulates tubular morphogenesis during repair from biliary damage in mice. *J Hepatol* 2013; **59**: 124-130 [PMID: 23500150 DOI: 10.1016/j.jhep.2013.02.025]

31 **Kohn A**, Dong Y, Mirando AJ, Jesse AM, Honjo T, Zuscik MJ, O'Keefe RJ, Hilton MJ. Cartilage-specific RBPjκ-dependent and -independent Notch signals regulate cartilage and bone development. *Development* 2012; **139**: 1198-1212 [PMID: 22354840 DOI: 10.1242/dev.070649]

32 **Zhang L**, Zhu C, Guo Y, Wei F, Lu J, Qin J, Banerjee S, Wang J, Shang H, Verma SC, Yuan Z, Robertson ES, Cai Q. Inhibition of

KAP1 enhances hypoxia-induced Kaposi's sarcoma-associated herpesvirus reactivation through RBP-Jκ. *J Virol* 2014; **88**: 6873-6884 [PMID: 24696491 DOI: 10.1128/JVI.00283-14]

33 **Hsieh JJ**, Nofziger DE, Weinmaster G, Hayward SD. Epstein-Barr virus immortalization: Notch2 interacts with CBF1 and blocks differentiation. *J Virol* 1997; **71**: 1938-1945 [PMID: 9032325]

34 **Mills CO**, Freeman JF, Salt PJ, Elias E. Effect of anaesthetic agents on bile flow and biliary excretion of 131I-cholylglycyltyrosine in the rat. *Br J Anaesth* 1989; **62**: 311-315 [PMID: 2784686 DOI: 10.1093/bja/62.3.311]

P- Reviewer: Abdel-Salam OM, Govindarajan GK, Silva ACS
S- Editor: Wang JL **L- Editor**: Filipodia **E- Editor**: Huang Y

Published by **Baishideng Publishing Group Inc**
7901 Stoneridge Drive, Suite 501, Pleasanton, CA 94588, USA
Telephone: +1-925-223-8242
Fax: +1-925-223-8243
E-mail: bpgoffice@wjgnet.com
Help Desk: http://www.f6publishing.com/helpdesk
http://www.wjgnet.com

ISSN 1007-9327